HHS Public Access

Author manuscript

Curr Protein Pept Sci. Author manuscript; available in PMC 2020 March 12.

Published in final edited form as:

Curr Protein Pept Sci. 2019 ; 20(12): 1189–1203. doi:10.2174/1389203720666190417120758.

Structure-based druggablity assessment of anti-virulence targets from Pseudomonas aeruginosa

Thamires Quadros Froes[a,b], **Regina Lúcia Baldini**[c], **Sandor Vajda**[d], **Marcelo Santos Castilho**[*,a,b]

[a]Programa de pós-graduação em Biotecnologia da Universidade Estadual de Feira de Santana, Feira de Santana, BA, Brazil.

[b]Faculdade de Farmácia da Universidade Federal da Bahia, Bahia, Salvador, BA, Brazil.

[c]Departamento de Bioquímica, Instituto de Química, Universidade de São Paulo. São Paulo, SP, Brazil.

[d]Department of Biomedical Engineering, Boston University, Boston, MA 02215, US

1. INTRODUCTION

The discovery of penicillin in the 20th century and the further development of other antibiotic therapies revolutionized medicine and contributed to longevity and quality of life[1] However, the increase in antimicrobial resistance (AMR) worldwide represents a serious threat to those achievements, as well as to public health[2]. Nowadays, approximately two million people are infected with antibiotic-resistant bacteria yearly in the USA[3], and about 25,000 people die every year in Europe, due to infections caused by drug-resistant bacteria [4]. The situation is even worse in low and middle-income countries where AMR claims the life of 214,000 newborns per year[5]. Apart from the huge impact on human lives, AMR also imposes high financial costs on patients and healthcare systems[6]. This scenario depicts an unmet medical need and a market opportunity for big pharma industries, however the interest in antibacterial research and development decreased significantly in the last decades. The underlying reasons for the antibacterial pipeline draught have been thoroughly discussed [7,8] and most authors agree that regulatory and economic issues, along with the fact that novel drugs might became useless within months due to AMR, are key components for the current lack of big pharma interest[9]. Therefore, very few novel classes of antibiotics have been discovered in the past couple of decades and the pipeline of agents under development is rather limited[10] (Figure 1).

Once regulatory guidelines are not expected to change nor antibiotic stewardship programs[11,12], overcoming AMR seems to be the only alternative to prevent apocalyptic predictions about the return of a “pre-antibiotic era” situation.[13]

[*]Address correspondence to this author at the Department of medicines, Faculty of Pharmacy, Federal University of Bahia, Salvador, Bahia; Tel/Fax: +55-71-99994-2643, +55-71-3283-6901; castilho@ufba.br.

CONFLICT OF INTEREST

none.

Although resistant bacteria have existed before the discovery and widespread prescription of antibacterial drugs, the evolutionary pressure caused by their introduction has significantly increased the number of resistant strains found in hospital settings and in the community[14,15]. Unfortunately, this is an expected consequence of their mechanisms of action, which often target bacterial growth or viability [16]. Although AMR has been the focus of thousands of publications in the last decades, this is still an unsolved problem that requires further research. For instance, an alternative approach to fight AMR is the search and/or design of anti-virulence drugs, which would decrease the aggressiveness of the pathogen towards the patient, but would not be affected by AMR, as these drugs would not target essential survival mechanisms [17,18].

Several excellent reviews[19,20,21,22] have already been published on this subject, but as far as we are aware, only one discusses the druggability of potential targets from a structure-based point of view[23]. Hence, this review paper aims at shedding light on this subject, explore recent advances on the field and highlight the importance of considering the druggability of putative targets during the drug design campaigns.

1.1. *Pseudomonas aeruginosa* as a model organism for anti-virulence drug development

Pseudomonas aeruginosa is a ubiquitous gram-negative bacterium with the ability to cause serious infections in humans. It can colonize burns and surgical wounds, it is a main cause of hospital-acquired infections, such as ventilator-associated pneumonia and poses a threat to cystic fibrosis patients[24-26]. *P. aeruginosa* infections are challenging to overcome, due to the intrinsic and acquired resistance mechanisms in action, including its outer membrane low permeability, numerous efflux pumps, expression of beta-lactamases, and growth in biofilms[27,28]. An increasing number of *P. aeruginosa* strains that are resistant to aminoglycosides, cephalosporins and quinolones has been observed in the last decade [4]. To make matters worse, there have been reports of *P. aeruginosa* clinical isolates that are resistant to all antipseudomonal drugs tested[29]. All these factors contribute to *P. aeruginosa* being included in the ESKAPE group of multi-resistant pathogens (*Enterococcus faecium, S. aureus, Klebsiella pneumoniae, Acinetobacter baumannii, P. aeruginosa,* and *Enterobacter* species)[30] and being included by the World Health Association in the global priority list of antibiotic-resistant bacteria to guide research, discovery, and development of new antibiotics [31,32].

Anti-virulence therapy has emerged as a promising alternative to overcome AMR in *P. aeruginosa* because this class of drugs would not lead to bacterial death or growth inhibition, as it is expected to pose a reduced selective pressure on the bacteria[20,22]. The expression of several virulence factors depends on cell-density regulated mechanisms, known as quorum sensing (QS) systems. In these systems, a small molecule, the auto-inducer (AI), is produced by the bacteria and, as the population increases, it reaches a concentration threshold that allows it to bind to a regulatory target, often a transcriptional activator, that turns on the expression of several genes, including virulence factors and other regulators, in a positive loop[33]. *P. aeruginosa* has three well-characterized QS systems, Las, Rhl and PQS, whose AIs and their molecular targets, the transcription factors LasR, QscR, RhlR and MvfR/PqsR have been extensively studied. More recently, a fourth system has been described as integrating

the QS hierarchy, but the molecular target of the novel AI IQS is still elusive[34,35]. Because the QS systems are crucial for the expression of a variety of virulence factors, including proteases, siderophores and secretion systems that target the host cells, they are promising targets for drug development[20]. Under QS regulation are also the genes which products are required for the synthesis of the phenazine pyocyanin, a secreted virulence factor that renders the *P. aeruginosa* cultures their blue-green appearance when the AI threshold is reached. Therefore, the production of pyocyanin is a useful marker of the functionality of the QS systems and it has been used for the characterization of QS inhibitors[36-40,41].

However, how druggable the QS targets are is a vital information that has been neglected in the search for anti-virulence compounds. The Aeropath database[42] was designed as a resource to aid the prioritization of targets from the genome of *P. aeruginosa* on overcome this knowledge gap. According to that database, only the transcriptional activator LasR and the enzyme PhzB2, which belongs to the pyocyanin biosynthetic pathway were druggable targets within the QS cascade. However, the discovery of nanomolar inhibitors of MvfR[43] and PqsD[44] suggests that the criteria employed by those authors were too stringent. The availability of a larger number of X-ray structures, updated genomic data and improved druggability prediction methods prompted us to revisit this subject and highlight how the information gathered from structure-based druggability assessment can be employed to guide the development of drugs to reduce *P. aeruginosa* virulence. In order to understand, in detail, the importance of answering this question, some concepts regarding druggability and its importance to drug-development campaigns are provided in the next section.

1.2. The relevance target druggability evaluation for anti-virulence drug development

Incorrect target selection has been considered a key component for the high attrition rate of several drug development projects [23,45,46] and several criteria have been employed to handpick high quality targets [47]. In general, the first requirement is that the macromolecular target takes part in a biochemical pathway that is responsible for the patient symptoms or for the cure, as is the case for infectious diseases. Accordingly, the first target selection criteria used considers how essential the protein is to bacterial survival. Gene knockout and RNA interference were largely employed to guide target selection at this level, but it soon became clear that not all essential targets are amenable to modulation by drug-like molecules. Moreover, anti-bacterial drug discovery programs that follow this model relies on screening assays that employ the minimal-inhibitory concentration (MIC) value as the selection criteria for hit identification and lead optimization. Obviously, the discovery of compounds that reduce the bacterial virulence, without affecting its viability, cannot follow this classical paradigm.

Another approach to select high quality targets relies on previous information from sequence-related or structure-related targets whose ligands are known[48]. As might be expected, the comparison of two highly conserved proteins, e.g. >70% sequence identity, shows that they bind to chemically related compounds and catalyze similar reactions. Consequently, ligands/inhibitors of the first protein should be useful to design ligands/inhibitors for the second one. Although this strategy proved to be very effective to well-studied targets, such as eukaryotic GPCRs, it is not very useful for innovative projects that

deal with scarcely explored biochemical pathways. The enzymes responsible for the pyocyanin biosynthesis, *per se*, can be included in this category. Another pitfall of this approach is that the entire sequence/structure is considered for target comparison, whereas the region where the ligand binds is composed of just a few residues in the structure (i.e. the active site). Thus, the druggability assessment or comparison of putative targets should consider only with the binding sites, not the whole protein tridimensional structure.

1.2. Structure-based assessment of anti-virulence targets in *P. aeruginosa*

Although the structure of several proteins that participate in the *P. aeruginosa* QS systems and pyocyanin biosynthesis pathway are available on the Protein Data Bank (PDB) (Tables 1-3), not all of them have their binding sites fully characterized. For instance, LasI, PhzB, PhzG, PhzM and PhzS were solved only with no ligand in the active site and PhzD had its sequence mutated to allow crystallization with the ligand (PhzD mutant PDB ID=1NF8).

In contrast, the X-ray structure of some targets have been solved in the presence of ligands/inhibitors: PDBind (http://www.pdbbind.org.cn/) has affinity data for five ligands that bind to four targets (MvfR, PqsE, PhzD and PhzF) whereas MOAD (http://bindingmoad.org/) shows data for just two of these targets (PhzD and PhzF). For these targets, identifying the binding site is straightforward. However, it is not so trivial to state how druggable the binding sites are, because some of the ligands have only micromolar potency towards their target (i.e. MvfR ligand QZN presents IC_{50}=5μM). The situation is complicated by the fact that most of these targets have no sequence-related structures available in PDB databank. PhzG might be considered an exception to that rule, once the X-ray structure of PhzG from *P. fluorescens* in complex with hexahydrophenazine-1,6-dicarboxylic acid (PDB ID: 4HMT -residues 18-222) and tetrahydrophenazine-1-carboxylic acid (PDB ID: 4HMV and 4HMU-(residues 20-222)) are available in PDB databank. However, the structure of *P. aeruginosa* PhzG (PDB ID: 1T9M), which accounts for residues 4-414 is apo.

In order to make a fair comparison of how easy it is to block the anti-virulence targets from *P. aeruginosa*, one could make use of *in silico* tools that ranks binding pockets according to their druggability.

1.3 *In silico* structure-based assessment of *P. aeruginosa* anti-virulence targets

The *in silico* approaches to identify putative binding pockets employ geometry- , information-, and/or energy-based algorithms[49]. Next, the putative pockets have their druggability ranked, mostly, according to their H-bonding ability, hydrophobicity profile and/or pocket volume [50,51,52,53,54; 55,56] . Druggability prediction models on known pockets affords good results[57]. However, the performance of models based on pocket estimation methods varies considerably[58,59]. In order to overcome this limitation, PockDrug-Server allows the user to employ either pre-defined pockets (from holo structures) or to use Fpocket to identify putative binding sites in the protein that will be classified as druggable or not, according to a model develop by Borrel et al.[58] (Figure 2). Briefly, the server employs a linear discriminant analysis, with 52 geometrical and physicochemical descriptors, to make a consensus prediction of the pocket druggability. According to the authors, druggable pockets

have an average 0.87 ± 0.15 score, whereas less-druggable pockets have an average of 0.18 ± 0.15 score [47].

In silico solvent mapping has also been employed for the identification of putative binding sites, as well as for their druggability assessment with high success rate[60,61,62]. FTMap is a freely available server that carries out solvent mapping by identifying low energy clusters of probe molecules (solvents) on protein surfaces. Wherever 16 or more probes are found together (Consensus site- CS), a hotspot that can be explored for drug design is present [60,63].

Hot spots can be defined as regions nearby residues that account for a significant change in binding affinity[62]. According to Kozakov and coworkers, the number of probes found in the CS is the first and foremost feature of a druggable binding site (S>16). Additional features include connectivity or compactness of the consensus sites (e.g. mean distance of 5-6 Å between CS centers) and the size of the hot spot region (<10 Å). Taking these three parameters into account, binding sites can be classified as: druggable using druglike compounds (D); not druggable due to weak hot spots (N); druggable only by large chemotype such as macrocycle or foldamer (DMF); druggable only by peptide, macrocycle, or charged compound (DPM); borderline druggable (at most micromolar affinity) using druglike compounds (BD); borderline druggable (micromolar affinity) by large chemotype such as macrocycle or foldamer (BMF) and borderline druggable (micromolar affinity) by peptide, macrocycle, or charged compound (BPM).

A major difference between these methods is that PockDrug employs an empirical method to predict how druggable is the binding site, whereas FTmap relies on physical principles to accomplish the same task. Each approach has its pros and cons, therefore targets that are considered as druggable by both software should provide a higher success rate in drug design campaigns. Accordingly, all proteins from *P. aeruginosa* involved in QS mechanisms or pyocyanin biosynthesis, with X-ray coordinates available in PDB databank, had their druggability predicted by these two approaches in this review paper (Figure 2). When no X-ray structure was available, homology-based models available in MOD base (https://modbase.compbio.ucsf.edu/modbase-cgi/index.cgi) were employed. This approach is supported by the work of Sarkar and Brenk which shows that structural homologues can be employed to predict the druggability of targets for which the X-ray structure is not available [23]. However, those authors have shown that sequence similarity, either global or in the active site, have no influence in the success rate of the druggability prediction. For this reason, the reader is advised to consider the predictions for homology models, presented in this review paper with caution.

The druggability assessment carried out with pockDrug and hot spots identified by FTmap are summarized in Tables 1-3 and discussed in the next sections, but it is worth mentioning that: 1) All QS receptors are considered druggable by PockDrug, but the classification according to hot spots criteria is a bit more variable (e.g. MvfR and QscR vary from DPM to D) (Table 1). As LasR and MvfR have been extensively explored as anti-virulence drug targets and they were classified mostly as druggable, section 4 will focus on how the information provided by these servers might be employed to improve the potency of available ligands; 2) LasI, PqsA and PqsD are deemed druggable by both servers, whereas

RhlI seems to be a difficult target (pockDrug= 0.5 ± 0.02 and FTmap= DPM). PqsE classification depends on the 3D structure employed for the analysis (Table 2). This variability might be due to conformational changes upon ligand binding, which allows a larger number of probes to bind to the CSs. Then, section 5 will focus on druggability predictions from apo structures and their reliability.

As mentioned before, several anti-virulence drug-design efforts rely on pyocyanin inhibition as a readout[64,65,66,67] , surprisingly very few efforts have been made to target enzymes that are responsible for the biosynthesis of this virulence factor. Therefore, the assessment of the pyocyanin biosynthetic enzymes as druggable targets remains to be determined. In order to shed some light on this subject, section 6 describes how pockDrug and FTmap results (Table 3) can be employed to select the best target(s) from this pathway and the challenges to design potent inhibitors for those targets.

1.3. Main druggable quorum sensing regulators from *P. aeruginosa*

The understanding of the mechanism of signal perception by the LuxR-type homo serine lactone (HSL) receptors has been largely been based on the structural data from TraRAt[68], QscR[69]102 as well as the HSL-binding domain from LasR[70] and the enteropathogenic *Escherichia coli* homologue SdiA[71]. These receptors are composed of two domains linked by a flexible loop which allows a variety of relative orientations for those domains. Like other LuxR proteins, LasR is stabilized by the ligand[72]. Then, all crystallographic data available was obtained either in the presence of HSL or an inhibitor molecule. In fact, LasR has received significant attention as a drug target due to its role in QS regulation[33,34]. PockDrug analysis shows that the substrate binding site is mainly hydrophobic (Kyte Hydrophobicity index= 0.64-0.78) and that the available volume for binding ranges from 2062.45 Å3 to 2325 Å3. Most of the hydrophobic interactions occur within the alkyl chain binding pocket, which is identified as the main hot spot in crystallographic structure of LasR in complex with 3-oxo-dodecanoyl-homoserine lactone (Figure 3- upper left panel). Although several homoserine lactones (HSL)-based antagonists[73] explore that hot spot and a consensus site nearby, the lactone ring not only is unstable at pH above 7, but it is also metabolized by mammalian lactonases[74,75]. Hence, this chemical scaffold poses several challenges for future drug development efforts.

The discovery of a different class of LasR agonists (TP1, Figure 3 - upper right panel)[76] brought some hope that antagonists could be developed from the initial hit. In order to achieve this goal, a series of triphenyl- derivatives was designed to further understand the chemical requirements for LasR modulation[77]. It has been shown that substituents in the ortho-position of ring A are required for LasR affinity and structural changes in the ring C are responsible for losing the agonist profile, no triphenyl derivative with potent LasR antagonist activity has been reported. The analysis of LasR hot spots, when TP1 is bound, suggests some modifications that might be explored to achieve this goal. For instance, addition of a substituent on position 5´ of ring C (*para* to NO_2 moiety). Although TP-1 derivatives bearing di and tri-substituted C-rings have already been synthesized, position 5´ was probed only with Fluor atom, which does not fully explore the hot spot region shown in Figure 3. Nevertheless, this derivative (number 34 in the original paper) shows a small

decrease in the agonist activity (TP1– 105% vs 34-89%) without significant change in the EC_{50} value (approx. 0.35 μM).

While the molecular basis for HSL-dependent QS on *P. aeruginosa* has long been studied[77], the alkyl quinolone (AQ)-type QS was discovered later[78]: 2-Heptyl-3-hydroxy-4(1H)-quinolone (commonly known as *Pseudomonas* Quinolone Signal, PQS) and its precursor (2-heptyl-4- hydroxyquinoline, HHQ) are the most important AQs responsible for MvfR activation[79, 80]. The fact that MvfR mutations lower *P. aeruginosa* virulence in animal infection models[81] and the presence of AQs in the sputum of patients with cystic fibrosis suggests that blockage of the AQ-type QS is a promising strategy to reduce *P. aeruginosa* virulence[82]. Initial efforts to achieve this goal either targeted enzymes that increased PQS metabolism[83] or that are responsible for its synthesis (see section 5).

An alternative target is the MvfR protein itself, which belongs to the LysR family of transcriptional regulators (LTTRs)[84, 85]. LTTR proteins generally possess a highly conserved DNA-binding domain but a poorly conserved ligand binding domain (LBD). Luckily, the LBD of MvfR has been solved both in apo form and in complex with several ligands[79,85]. The X-ray structure of MvfR LBD in complex with NHQ reveals that the substrate occupies two different pockets: the quinolone pocket is composed of Tyr258, Ile186, Val170, Leu189 and Ile236 and the alkyl-chain pocket is lined by Leu207, Leu208, Ile236, Ile149, Ala168 and Phe221. Those two pockets have 1603.42 Å3 volume and a Kyte Hydrophobicity index=2.59, according to the PockDrug server. These features along with frequency of polar (0.16) and aromatic (0.11) residues guarantee the highest druggability score for this target.

FTmap analysis not only confirms that prediction but also shows that alkyl-chain binds to the strongest hot spot (S=23) whereas the quinolone rings reaches another hot spot (19 probes) that is located within 5.39Å (center to center) distance (Figure 4 - lower left panel). Modifications in the quinolone ring afforded compounds with antagonist activity such as 3-amino-7-chloro-2-nonylquinazolin-4(3H)-one[79] and the benzoimidazole derivative M6443, which bioactive conformation takes advantage of all hot spots within MvfR binding site (Figure 3- lower right panel). As expected, this compound has high affinity towards its macromolecular target.

Hot spots strength and location change according to the structural flexibility of the protein. Hence, the true impact of the information provided by PockDrug and FTmap is best evaluated if apo structures are employed for the analysis. In order to highlight the strengths and limitations of such approach, the next section not only describes druggable targets that are responsible for either HSL or PQS biosynthesis, but also discusses if those targets would be considered as druggable if just apo structures were considered.

1.4. Druggable targets within HSL and PQS biosynthetic pathways: opportunities and limitations of structure-based *in silico* druggability prediction methods.

Among the three HSL synthase families identified so far (LuxI, HdtS, and LuxM), LuxI is the most common in Gram-negative bacteria and the two *P. aeruginosa* HSL synthases, LasI and RhlI, belong to this family .35,75. Before the X-ray structures of EsaI (PDB ID= 1K4J) LasI (PDB ID= 1RO5) and TofI (PDB ID=3P2H and 3P2F(APO), the role of individual

residues in the substrate recognition and catalysis were based on mutational analyses[86, 87]. Nowadays, it is known that Arg23, Glu42, Asp44, Asp47, Arg70, Arg104 and Gly68 are involved in S-adenosylmethionine (SAM) recognition, whereas the acyl-chain binding site is formed by Met79, Phe105, Thr142 and Thr144[88]. Differences in hydrophobic side chains sizes as well as minor rearrangements in α6 and α8 orientation might explain the closed acyl-chain pocket in EsaI versus the "tunnel"-like binding site proposed for LasI. However, it has been argued that such tunnel is not accessible and that the real acyl-chain binding site is yet to be identified[89]. Although this point requires further investigation, the availability of the LasI structure in the apo form allows PockDrug and FTmap to be employed in a real-life situation that mimics the early stages of drug developments campaigns. For instance, structural overlay of LasI (apo) and TofI (holo) (Figure 4) shows that loop 30–36 shifts to a closed conformation when SAM is absent. Hence, hot spots in that region would not be predicted correctly from the apo structure. Moreover, the success rate of binding site identification has a direct impact on how useful the druggability assessment really is. Taking these points into consideration, Pockdrug server predicts LasI to have one pocket with at least 14 residues (P0 volume 1306.24 Å3), two pockets with 10–14 residues (volume= P1 462.13 and P4 536.05 Å3) and three decoy pockets. The substrate binding site is formed by residues from P0 (Druggability score= 1.0) and P1 (Druggability score= 0.92 ± 0.05), which are considered as druggable (Table 2).

FTmap supports that classification, because the first hot spot (S=24) is located 7.05 Å (center-to-center distance) from the second hot spot and both of them are within this pocket (Figure 4). In contrast to LasR, the hot spots on LasI do not overlap the alkyl-chain of the HSL. This suggests that the chemical features of LasI inhibitors should be quite different from a LasR antagonist, despite both macromolecules bind HSL. The reader should not consider this as hard-evidence about the chemical differences of LasR antagonists and LasI inhibitors, although molecules that bind the first have never been reported to inhibit the second and vice-versa.

Instead of a single step, the synthesis of PQS requires five enzymes that are encoded in the *pqsABCDE* operon[90]. The PQS biosynthesis starts from anthranilic acid which is linked to acetyl-CoA by PqsA. This intermediate is then condensed to malonyl-CoA, by the action of PqsD and the unstable product of that reaction is hydrolyzed to 2-aminobenzoylacetate (2-ABA) by PqsE. Next, the PqsB-PqsC hetero complex builds the quinolone core from 2-ABA and octanoyl-CoA to afford HHQ. After that, PqsH adds a hydroxyl moiety to the position 3 of the quinolone scaffold.[90]

The fact that knockout mutants lacking PqsA show attenuated virulence in acute murine infection models as well as reduced biofilm formation[91] along with the consensus classification of this macromolecule as a druggable target by pockdrug and FTmap, strongly suggests that PqsA inhibitors may have a huge impact on the virulence of *P. aeruginosa*.

In contrast, the PqsE druggability score, according to PockDrug, is close to the minimum acceptable value for a druggable target. FTmap druggability classification for this target varies from non-druggable to druggable, depending on which X-ray structure is employed for analysis. As pointed out before, this wide classification variability is due to

conformational changes that either exposes hidden hot spots or bring them closer together. As a consequence, PqsE seems to be a trick target, whose structure-based druggability assessment, at this point, is highly speculative.

1.5. Unexplored druggable targets from pyocyanin biosynthesis pathway

Pyocyanin (PYO) is a blue-green pigment from *Pseudomonas aeruginosa* that is involved in the regulation of ion transport, bacterial cell movement, redox balance as well as host immune response through the modulation of cytokines expression and mucus secretion in the airways [92-95]. In fact, acute and chronic lung infection models in mice show that bacteria survival is reduced when PYO biosynthesis is impaired[96]. Thus, pyocyanin plays a pivotal role in P. aeruginosa virulence and inhibiting its biosynthesis has been accomplished by modulation of QS targets. It is quite surprising that the enzymes responsible for the biosynthesis of this pigment have received much less attention[97], despite all the knowledge that has been accumulated in the last decade. From a genetic point of view, the biosynthesis can be split in two parts; first the genes found in two homologous operons (phzA1B1C1D1E1F1G1 and phzA2B2C2D2E2F2G2) encode the enzymes responsible for PCA synthesis. Then, PhzM and PhzS, which are coded by separated genes[98] carry out the final steps of pyocyanin biosynthesis. From a biochemical perspective, PYO biosynthesis begins with the conversion the chorismic acid to 2-amino-4-deoxychorismic acid (ADIC) by PhzE[99]. ADIC is then reduced to 2,3-dihydro-3-hydroxyanthranilic acid (DHHA) by PhzD)[100]. Next, PhzF catalyzes the isomerization of DHHA to (1R,6S)-6-amino-5-oxocyclohex-2-ene-1 carboxylic acid (AOCHC) via (1 R,6S)-6-amino-5-hydroxy-2,4-cyclohexene-1-carboxylic acid (AOCHC) by [1,5]-hydrogen shift followed by a stereospecific tautomerization step[101]. The condensation of two AOCHC molecules, catalyzed by PhzB, affords the unstable intermediate hexahydrophenazine-1,6-dicarboxylic acid (HHPDC), which undergoes rapid oxidative decarboxylation to produce tetrahydrophenazine-1,6-carboxylic acid (THPCA)[102]. The last step in the synthesis of the phenazine nucleus is carried out by PhzG[103]. Then, phenazine-1-carboxylic acid (PCA) is converted to pyocyanin (PYO) by the concerted action of PhzM and PhzS[104]. When PhzM is absent (or inhibited), PCA can either be converted to phenazine-1-carboxamide by PhzH, or PCA to 1-hydrophenazine by the action of PhzS[104]. Several of those enzymes have their X-ray structure available in the PDB databank and one of the reasonable explanations for not exploring this biochemical pathway to develop anti-virulence drugs is the lack of studies regarding the druggability of the putative targets. One exception to that rule is PhzB2, which has been suggested to be a druggable target [23]. Taking all this information into consideration, the following paragraphs explore the druggable targets from this pathway, according to PockDrug server and FTmap hot spot criteria (Table 3).

Although the coordinates of PhzB from *P. aeruginosa* are available in the PDB databank (PDB ID 3FF0), the details of this crystallographic structure have never been published. As a consequence, most of the date presented next are derived from the crystallographic structure of PhzA/B from *Burkholderia cepacia* R18194 [102].These enzymes share 62% sequence identity, and both have a large central cavity where the substrate binds. According to PockDrug, the binding site has approximately 3435.91 Å3 and a Kyte hydrophobicity index=0.23, if only one monomer is employed for the calculation. However, PhzB is a

dimeric enzyme, whose C-terminal residues from chain A may occlude the binding site of the other subunit, during catalysis, and thus increase the hydrophobicity. In the absence of the substrate, this flexible-lid is disordered. So it seems reasonable to employ just one monomer for the druggability assessment described here. The hot spot with highest number of probes (S= 24) overlaps with the position of an unknown electron density within the *P. aeruginosa* PhzB binding site (Figure 5), which is compatible to a benzoic acid (or nitro-benzene), according to the remark in the PDB entry. Next to this location, there is another hot spot (5.74Å center-to-center distance) that would allow a drug-like molecule to bind with high affinity to PhzB. The analysis of the residues surrounding these two hot spots reveals that a putative ligand might be anchored by hydrophobic interactions to Leu50, Ile61, Trp73m Phe78 and Phe121, whereas H-bonds to His70, Glu137 (major hot spot) and/or Tyr117 might be explored to increase its selectivity.

The second druggable target, according to pockDRug server and Hot spot criteria is PhzD. This enzyme has a buried active site at the C-terminal end of a β-sheet and near the dimer interface[105]. The crystal structure of the mutant D38A in complex with isochorismate reveals the substrate is hold into place by hydrophobic interactions to I4, W94, F43, Y125, Y151, L154 and F180, whereas Q78, R87, G155, Y151 and K122 form hydrogen bonds[105]. Overall, the binding site is smaller and less hydrophobic than the one in PhzB (1304.28 Å vs 3435.91 Å and kyte hydrophobicity index= −0.07 vs 0.23). As a consequence, FTmap does not identify hot spots within the binding site and it suggests that by peptide-like, macrocycles or charged compounds might bind to a superficial pocket in the protein surface (Figure 6).

Therefore, PhzD is a classic example of binding site prediction mismatch. In case the user explicitly tells FTmap where to look for hot spots (around the ligand), the software finds a strong one (S=20) that overlaps with the carboxy-vinyl moiety at position 5 of the cyclohexadiene ring. A secondary hot spot (5 probes), located 7.57 Å (center-to-center distance) from the first, overlaps with the hydroxyl at position 6 and suggests that blocking the binding site entrance is the best strategy to inhibit PhzD. This strategy might have the additional benefit of disrupting the protein-protein interaction network, due to the binding site location at the dimer interface.

CONCLUSION

Structure-based druggability assessment of anti-virulence targets is an invaluable tool to select suitable targets for drug development efforts. When this strategy is employed along with *in silico* solvent mapping, additional information is provided, for instance, which chemical modifications can be made to better explore the hotspots within the binding site. However, both FTmap-based nor Pockdrug-based approaches have limitations that might be minimized by consensus prediction of the targets druggability. The examples described in this review highlight some, but not all, of the insights provided by PockDrug and FTmap servers towards the development of anti-virulence drugs, which shall be useful to overcome the worldwide antimicrobial resistance issue.

REFERENCES

(1). Ventola CL The Antibiotic Resistance Crisis: Part 1: Causes and Threats. P T A peer-reviewed J. Formul. Manag 2015, 40 (4), 277–283.

(2). Report, G. Antimicrobial Resistance. 2014.

(3). Antibiotic Use in the United States, 2017: Progress and Opportunities.

(4). ECDC. Antimicrobial Resistance Surveillance in Europe 2015. Annual Report of the European Antimicrobial Resistance Surveillance Network (EARS-Net).; 2015.

(5). Singh SB; Young K; Silver LL What Is an “Ideal” Antibiotic? Discovery Challenges and Path Forward. Biochemical Pharmacology. 2017.

(6). Thorpe KE; Joski P; Johnston KJ Antibiotic-Resistant Infection Treatment Costs Have Doubled since 2002, Now Exceeding $2 Billion Annually. Health Aff. 2018, 37 (4), 662–669.

(7). Fedorenko V; Genilloud O; Horbal L; Marcone GL; Marinelli F; Paitan Y; Ron EZ Antibacterial Discovery and Development: From Gene to Product and Back. BioMed Research International. 2015.

(8). Fernandes P; Martens E Antibiotics in Late Clinical Development. Biochemical Pharmacology. 2017.

(9). Tacconelli E; Carrara E; Savoldi A; Harbarth S; Mendelson M; Monnet DL; Pulcini C; Kahlmeter G; Kluytmans J; Carmeli Y; et al. Articles Discovery, Research, and Development of New Antibiotics: The WHO Priority List of Antibiotic-Resistant Bacteria and Tuberculosis.

(10). Bush K; Page MGP What We May Expect from Novel Antibacterial Agents in the Pipeline with Respect to Resistance and Pharmacodynamic Principles. J. Pharmacokinet. Pharmacodyn 44.

(11). Jump RLP; Gaur S; Katz MJ; Crnich CJ; Dumyati G; Ashraf MS; Frentzel E; Schweon SJ; Sloane P; Nace D Template for an Antibiotic Stewardship Policy for Post-Acute and Long-Term Care Settings. J. Am. Med. Dir. Assoc 2017, 18 (11), 913–920. [PubMed: 28935515]

(12). Rogers Van Katwyk S; Grimshaw JM; Mendelson M; Taljaard M; Hoffman SJ Government Policy Interventions to Reduce Human Antimicrobial Use: Protocol for a Systematic Review and Meta-Analysis. Syst. Rev 2017, 6 (1), 1–10. [PubMed: 28077170]

(13). Defoirdt T Quorum-Sensing Systems as Targets for Antivirulence Therapy. Trends in Microbiology. 2018.

(14). Zucca M; Scutera S; Savoia D New Antimicrobial Frontiers. Mini Rev Med Chem 2011, 888–900. [PubMed: 21781024]

(15). Heras B; Scanlon MJ; Martin JL Targeting Virulence Not Viability in the Search for Future Antibacterials. Br. J. Clin. Pharmacol 2015, 79 (2), 208–215. [PubMed: 24552512]

(16). Fair RJ; Tor Y Perspectives in Medicinal Chemistry Antibiotics and Bacterial Resistance in the 21st Century. Perspect. Medicin. Chem 2014, 25–64. [PubMed: 25232278]

(17). Dickey_2017_NAture.

(18). Johnson BK; Abramovitch RB Small Molecules That Sabotage Bacterial Virulence. Trends Pharmacol. Sci 2017, 38 (4), 339–362. [PubMed: 28209403]

(19). Cui Q; Lv H; Qi Z; Jiang B; Xiao B; Liu L; Ge Y; Hu X Cross-Regulation between the Phz1 and Phz2 Operons Maintain a Balanced Level of Phenazine Biosynthesis in Pseudomonas Aeruginosa PAO1. PLoS One 2016, 11 (1), 1–20.

(20). Maura D; Ballok AE; Rahme LG Considerations and Caveats in Anti-Virulence Drug Development. Current Opinion in Microbiology. 2016.

(21). Czaplewski L; Bax R; Clokie M; Dawson M; Fairhead H; Fischetti VA; Foster S; Gilmore BF; Hancock REW; Harper D; et al. Alternatives to Antibiotics-a Pipeline Portfolio Review. The Lancet Infectious Diseases. 2016.

(22). DIckey SW; Cheung GYC; Otto M Different Drugs for Bad Bugs: Antivirulence Strategies in the Age of Antibiotic Resistance. Nature Reviews Drug Discovery. 2017.

(23). Sarkar A; Brenk R To Hit or Not to Hit, That Is the Question -Genome-Wide Structure-Based Druggability Predictions for Pseudomonas Aeruginosa Proteins. PLoS One 2015, 10 (9), 1–16.

(24). Lyczak JB; Cannon CL; Pier GB Establishment of Pseudomonas Aeruginosa Infection: Lessons from a Versatile Opportunist. Microbes Infect 2000, 2 (9), 1051–1060. [PubMed: 10967285]

(25). Wagner VE; Iglewski BH P. Aeruginosa Biofilms in CF Infection. Clin Rev Allergy Immunol 2008.

(26). Gaynes R; Edwards JR Overview of Nosocomial Infections Caused by Gram-Negative Bacilli.

(27). Breidenstein EB; de la Fuente-Nunez C; Hancock RE Pseudomonas Aeruginosa: All Roads Lead to Resistance. Trends Microbiol 2011, 19 (8), 419–426. [PubMed: 21664819]

(28). Taylor PK; Yeung ATY; Hancock REW Antibiotic Resistance in Pseudomonas Aeruginosa Biofilms: Towards the Development of Novel Anti-Biofilm Therapies. J. Biotechnol 2014, 191, 121–130. [PubMed: 25240440]

(29). Theuretzbacher U Global Antimicrobial Resistance in Gram-Negative Pathogens and Clinical Need. Current Opinion in Microbiology. 2017.

(30). Rice LB Federal Funding for the Study of Antimicrobial Resistance in Nosocomial Pathogens: No ESKAPE. J. Infect. Dis 2008, 197 (8), 1079–1081. [PubMed: 18419525]

(31). Kahlmeter G; Singh N GLOBAL PRIORITY LIST OF ANTIBIOTIC-RESISTANT BACTERIA TO GUIDE RESEARCH, DISCOVERY, AND DEVELOPMENT OF NEW ANTIBIOTICS.

(32). Tacconelli E; Carrara E; Savoldi A; Harbarth S; Mendelson M; Monnet DL; Pulcini C; Kahlmeter G; Kluytmans J; Carmeli Y; et al. Discovery, Research, and Development of New Antibiotics: The WHO Priority List of Antibiotic-Resistant Bacteria and Tuberculosis. Lancet Infect. Dis 2018, 18 (3), 318–327. [PubMed: 29276051]

(33). Rutherford ST; Bassler BL Bacterial Quorum Sensing: Its Role in Virulence and Possibilities for Its Control. Cold Spring Harb. Perspect. Med 2012, 2 (11), a012427–a012427. [PubMed: 23125205]

(34). Lee J; Zhang L The Hierarchy Quorum Sensing Network in Pseudomonas Aeruginosa. Protein Cell 2014, 6 (1), 26–41. [PubMed: 25249263]

(35). Lee J; Wu J; Deng Y; Wang J; Wang C; Wang J; Chang C; Dong Y; Williams P; Zhang L-H A Cell-Cell Communication Signal Integrates Quorum Sensing and Stress Response. Nat. Chem. Biol 2013, 9 (5), 339–343. [PubMed: 23542643]

(36). O'Loughlin CT; Miller LC; Siryaporn A; Drescher K; Semmelhack MF; Bassler BL A Quorum-Sensing Inhibitor Blocks Pseudomonas Aeruginosa Virulence and Biofilm Formation. Proc. Natl. Acad. Sci 2013, 110 (44), 17981–17986. [PubMed: 24143808]

(37). Luo J; Dong B; Wang K; Cai S; Liu T; Cheng X; Lei D; Chen Y; Li Y; Kong J; et al. Baicalin Inhibits Biofilm Formation, Attenuates the Quorum Sensing-Controlled Virulence and Enhances Pseudomonas Aeruginosa Clearance in a Mouse Peritoneal Implant Infection Model. PLoS One 2017, 12 (4), e0176883. [PubMed: 28453568]

(38). Al-Yousef HM; Ahmed AF; Al-Shabib NA; Laeeq S; Khan RA; Rehman MT; Alsalme A; Al-Ajmi MF; Khan MS; Husain FM Onion Peel Ethylacetate Fraction and Its Derived Constituent Quercetin 4′-O-β-D Glucopyranoside Attenuates Quorum Sensing Regulated Virulence and Biofilm Formation. Front. Microbiol 2017, 8, 1675. [PubMed: 28928721]

(39). Heidari A; Noshiranzadeh N; Haghi F; Bikas R Inhibition of Quorum Sensing Related Virulence Factors of Pseudomonas Aeruginosa by Pyridoxal Lactohydrazone. Microb. Pathog 2017, 112, 103–110. [PubMed: 28939255]

(40). Chatterjee M; D'Morris S; Paul V; Warrier S; Vasudevan AK; Vanuopadath M; Nair SS; Paul-Prasanth B; Mohan CG; Biswas R Mechanistic Understanding of Phenyllactic Acid Mediated Inhibition of Quorum Sensing and Biofilm Development in Pseudomonas Aeruginosa. Appl. Microbiol. Biotechnol 2017, 101 (22), 8223–8236. [PubMed: 28983655]

(41). Papenfort K; Bassler BL Quorum Sensing Signal-Response Systems in Gram-Negative Bacteria. Nat. Rev. Microbiol 2016, 14 (9), 576–588. [PubMed: 27510864]

(42). Moynie L; Schnell R; McMahon SA; Sandalova T; Boulkerou WA; Schmidberger JW; Alphey M; Cukier C; Duthie F; Kopec J; et al. The AEROPATH Project Targeting Pseudomonas Aeruginosa: Crystallographic Studies for Assessment of Potential Targets in Early-Stage Drug Discovery. Acta Crystallogr. Sect. F Struct. Biol. Cryst. Commun 2013, 69 (1), 25–34.

(43). Starkey M; Lepine F; Maura D; Bandyopadhaya A; Lesic B; He J; Kitao T; Righi V; Milot S; Tzika A; et al. Identification of Anti-Virulence Compounds That Disrupt Quorum-Sensing Regulated Acute and Persistent Pathogenicity. PLoS Pathog. 2014.

(44). Hinsberger S; de Jong JC; Groh M; Haupenthal J; Hartmann RW Benzamidobenzoic Acids as Potent PqsD Inhibitors for the Treatment of Pseudomonas Aeruginosa Infections. Eur. J. Med. Chem 2014, 76, 343–351. [PubMed: 24589489]

(45). Payne DJ; Gwynn MN; Holmes DJ; Pompliano DL Drugs for Bad Bugs: Confronting the Challenges of Antibacterial Discovery. Nat. Rev. Drug Discov 2007, 6 (1), 29–40. [PubMed: 17159923]

(46). Agüero F; Al-lazikani B; Aslett M; Berriman M; Frederick S; Campbell RK; Carmona S; Carruthers IM; Edith a W.; Chen F; et al. Database. 2008, 7 (11), 900–907.

(47). Abi Hussein H; Geneix C; Petitjean M; Borrel A; Flatters D; Camproux AC Global Vision of Druggability Issues: Applications and Perspectives. Drug Discov. Today 2017, 22 (2), 404–415. [PubMed: 27939283]

(48). Fauman EB; Rai BK; Huang ES Structure-Based Druggability Assessment-Identifying Suitable Targets for Small Molecule Therapeutics. Curr. Opin. Chem. Biol 2011, 15 (4), 463–468. [PubMed: 21704549]

(49). Vukovic S; Huggins DJ Quantitative Metrics for Drug–Target Ligandability. Drug Discov. Today 2018, 23 (6), 1258–1266. [PubMed: 29522887]

(50). Sheridan RP; Maiorov VN; Holloway MK; Cornell WD; Gao Y-D Drug-like Density: A Method of Quantifying the "Bindability" of a Protein Target Based on a Very Large Set of Pockets and Drug-like Ligands from the Protein Data Bank. J. Chem. Inf. Model 2010, 50 (11), 2029–2040. [PubMed: 20977231]

(51). Seco J; Luque FJ; Barril X Binding Site Detection and Druggability Index from First Principles. J. Med. Chem 2009, 52 (8), 2363–2371. [PubMed: 19296650]

(52). Halgren TA Identifying and Characterizing Binding Sites and Assessing Druggability. J. Chem. Inf. Model 2009, 49 (2), 377–389. [PubMed: 19434839]

(53). Krasowski A; Muthas D; Sarkar A; Schmitt S; Brenk R DrugPred: A Structure-Based Approach to Predict Protein Druggability Developed Using an Extensive Nonredundant Data Set. J. Chem. Inf. Model 2011, 51 (11), 2829–2842. [PubMed: 21995295]

(54). Nisius B; Sha F; Gohlke H Structure-Based Computational Analysis of Protein Binding Sites for Function and Druggability Prediction. J. Biotechnol 2012, 159 (3), 123–134. [PubMed: 22197384]

(55). Perola E; Herman L; Weiss J Development of a Rule-Based Method for the Assessment of Protein Druggability. J. Chem. Inf. Model 2012, 52 (4), 1027–1038. [PubMed: 22448735]

(56). Volkamer A; Kuhn D; Grombacher T; Rippmann F; Rarey M Combining Global and Local Measures for Structure-Based Druggability Predictions. J. Chem. Inf. Model 2012, 52 (2), 360–372. [PubMed: 22148551]

(57). Desaphy J; Azdimousa K; Kellenberger E; Rognan D Comparison and Druggability Prediction of Protein-Ligand Binding Sites from Pharmacophore-Annotated Cavity Shapes. J. Chem. Inf. Model 2012, 52 (8), 2287–2299. [PubMed: 22834646]

(58). Borrel A; Regad L; Xhaard H; Petitjean M; Camproux AC PockDrug: A Model for Predicting Pocket Druggability That Overcomes Pocket Estimation Uncertainties. J. Chem. Inf. Model 2015, 55 (4), 882–895. [PubMed: 25835082]

(59). Hussein HA; Borrel A; Geneix C; Petitjean M; Regad L; Camproux AC PockDrug-Server: A New Web Server for Predicting Pocket Druggability on Holo and Apo Proteins. Nucleic Acids Res. 2015, 43 (W1), W436–W442. [PubMed: 25956651]

(60). Brenke R; Kozakov D; Chuang GY; Beglov D; Hall D; Landon MR; Mattos C; Vajda S Fragment-Based Identification of Druggable “hot Spots” of Proteins Using Fourier Domain Correlation Techniques. Bioinformatics 2009, 25 (5), 621–627. [PubMed: 19176554]

(61). Grove LE; Hall DR; Beglov D; Vajda S; Kozakov D FTFlex: Accounting for Binding Site Flexibility to Improve Fragment-Based Identification of Druggable Hot Spots. Bioinformatics 2013, 29 (9), 1218–1219. [PubMed: 23476022]

(62). Kozakov D; Hall DR; Napoleon RL; Yueh C; Whitty A; Vajda S New Frontiers in Druggability. Journal of Medicinal Chemistry. 2015.

(63). Kozakov D; Grove LE; Hall DR; Bohnuud T; Mottarella S; Luo L; Xia B; Beglov D; Vajda S HHS Public Access. 2016, 10 (5), 733–755.

(64). Forezi LSM; Froes TQ; Cardoso MFC; De Oliveira Maciel CA; Nicastro GG; Baldini RL; Costa DCS; Ferreira VF; Castilho MS; Da Silva FC Synthesis and Biological Evaluation of Coumarins Derivatives as Potential Inhibitors of the Production of Pseudomonas Aeruginosa Virulence Factor Pyocyanin. Curr. Top. Med. Chem 2018, 18 (2).

(65). Sui SJH; Lo R; Fernandes AR; Caulfield MDG; Lerman JA; Xie L; Bourne PE; Baillie DL; Fiona SL; Jolla L; et al. HHS Public Access. 2012, 40 (3), 246–251.

(66). Zhao ZG; Yan SS; Yu YM; Mi N; Zhang LX; Liu J; Li XL; Liu F; Xu JF; Yang WQ; et al. An Aqueous Extract of Yunnan Baiyao Inhibits the Quorum-Sensing-Related Virulence of Pseudomonas Aeruginosa. J. Microbiol 2013, 51 (2), 207–212. [PubMed: 23625222]

(67). Morkunas B; Gal B; Galloway WRJD; Hodgkinson JT; Ibbeson BM; Tan YS; Welch M; Spring DR Discovery of an Inhibitor of the Production of the Pseudomonas Aeruginosa Virulence Factor Pyocyanin in Wild-Type Cells. 2016, 1428–1433.

(68). Vannini A; Volpari C; Gargioli C; Muraglia E; Cortese R; Francesco R. De; Neddermann P; Marco S. Di. The Crystal Structure of the Quorum Sensing Protein TraR Bound to Its Autoinducer and Target DNA. 2002, 21 (17), 4393–4401.

(69). Lintz MJ; Oinuma K-I; Wysoczynski CL; Greenberg EP; Churchill MEA Crystal Structure of QscR, a Pseudomonas Aeruginosa Quorum Sensing Signal Receptor. Proc. Natl. Acad. Sci 2011, 108 (38), 15763–15768. [PubMed: 21911405]

(70). Bottomley MJ; Muraglia E; Bazzo R; Carfı A Molecular Insights into Quorum Sensing in the Human Pathogen Pseudomonas Aeruginosa from the Structure of the Virulence Regulator LasR Bound to Its Autoinducer *. 2007, 282 (18), 13592–13600.

(71). Yao Y; Martinez-yamout MA; Dickerson TJ; Brogan AP; Wright PE; Dyson HJ Structure of the Escherichia Coli Quorum Sensing Protein SdiA : Activation of the Folding Switch by Acyl Homoserine Lactones. 2006, 262–273.

(72). Lamb JR; Patel H; Montminy T; Wagner VE; Iglewski BH; Acteriol JB Functional Domains of the RhlR Transcriptional Regulator of Pseudomonas Aeruginosa. 2003, 185 (24), 7129–7139.

(73). Geske. Reveals a New Set of Potent Quorum Sensing Modulators. 2009, 18 (22), 5978–5981.

(74). Ozer EA; Pezzulo A; Shih DM; Chun C; Furlong C; Lusis AJ; Greenberg EP; Zabner J Human and Murine Paraoxonase 1 Are Host Modulators of Pseudomonas Aeruginosa Quorum-Sensing. FEMS Microbiol. Lett 2005, 253 (1), 29–37. [PubMed: 16260097]

(75). Yang F; Wang LH; Wang J; Dong YH; Hu J; Zhang LH Quorum Quenching Enzyme Activity Is Widely Conserved in the Sera of Mammalian Species. FEBS Lett. 2005, 579 (17), 3713–3717. [PubMed: 15963993]

(76). Schuster M; Heim R; Singh A; Olson ER; Greenberg EP Novel Pseudomonas Aeruginosa Quorum-Sensing Inhibitors Identified in an Ultra-High-Throughput Screen †. 2006, 50 (11), 3674–3679.

(77). Capilato JN; Philippi SV; Reardon T; McConnell A; Oliver DC; Warren A; Adams JS; Wu C; Perez LJ Development of a Novel Series of Non-Natural Triaryl Agonists and Antagonists of the Pseudomonas Aeruginosa LasR Quorum Sensing Receptor. Bioorganic Med. Chem 2017, 25 (1), 153–165.

(78). Pesci EC; Milbank JBJ; Pearson JP; McKnight S; Kende AS; Greenberg EP; Iglewski BH Quinolone Signaling in the Cell-to-Cell Communication System of Pseudomonas Aeruginosa. Proc. Natl. Acad. Sci 1999, 96 (20), 11229–11234. [PubMed: 10500159]

(79). Ilangovan A; Fletcher M; Rampioni G; Pustelny C; Rumbaugh K; Heeb S; Cámara M; Truman A; Chhabra SR; Emsley J; et al. Structural Basis for Native Agonist and Synthetic Inhibitor Recognition by the Pseudomonas Aeruginosa Quorum Sensing Regulator PqsR (MvfR). PLoS Pathog. 2013, 9 (7).

(80). Ortori CA; Dubern JF; Chhabra SR; Cámara M; Hardie K; Williams P; Barrett DA Simultaneous Quantitative Profiling of N-Acyl-l-Homoserine Lactone and 2-Alkyl-4(1H)-Quinolone Families of Quorum-Sensing Signaling Molecules Using LC-MS/MS. Anal. Bioanal. Chem 2011, 399 (2), 839–850. [PubMed: 21046079]

(81). Cao H; Krishnan G; Goumnerov B; Tsongalis J; Tompkins R; Rahme LG A Quorum Sensing-Associated Virulence Gene of Pseudomonas Aeruginosa Encodes a LysR-like Transcription

Regulator with a Unique Self-Regulatory Mechanism. Proc Natl Acad Sci U S A 2001, 98 (25), 14613–14618. [PubMed: 11724939]

(82). Collier DN; Anderson L; Mcknight SL; Noah TL; Knowles M; Boucher R; Schwab U; Gilligan P; Pesci EC A Bacterial Cell to Cell Signal in the Lungs of Cystic ¢ Brosis Patients. 2002, 215, 41–46.

(83). Pustelny C; Albers A; Büldt-Karentzopoulos K; Parschat K; Chhabra SR; Cámara M; Williams P; Fetzner S Dioxygenase-Mediated Quenching of Quinolone-Dependent Quorum Sensing in Pseudomonas Aeruginosa. Chem. Biol 2009, 16 (12), 1259–1267. [PubMed: 20064436]

(84). Kefala K; Kotsifaki D; Providaki M; Kapetaniou EG; Rahme L; Kokkinidis M Purification, Crystallization and Preliminary X-Ray Diffraction Analysis of the C-Terminal Fragment of the MvfR Protein from Pseudomonas Aeruginosa. Acta Crystallogr. Sect. F Struct. Biol. Cryst. Commun 2012, 68 (6), 695–697.

(85). Kitao T; Lepine F; Babloudi S; Walte F; Steinbacher S; Maskos K; Blaesse M; Negri M; Pucci M; Zahler B; et al. Molecular Insights into Function and Competitive Inhibition of Pseudomonas Aeruginosa Multiple Virulence Factor Regulator. MBio 2018.

(86). Parsek MR; Schaefer a L.; Greenberg EP Analysis of Random and Site-Directed Mutations in RhII, a Pseudomonas Aeruginosa Gene Encoding an Acylhomoserine Lactone Synthase. Mol. Microbiol 1997, 26 (2), 301–310. [PubMed: 9383155]

(87). Hanzelka BL; Stevens, a M.; Parsek, M. R.; Crone, T. J.; Greenberg, E. P. Mutation Analysis of the Vibrio Fisceri LuxI Polypeptide:Critical Regions of an Autoinducer Synthase. J. Bacteriol 1997, 179 (15), 4882–4887. [PubMed: 9244278]

(88). Gould TA; Schweizer HP; Churchill MEA Structure of the Pseudomonas Aeruginosa Acyl-Homoserinelactone Synthase LasI. Mol. Microbiol 2004, 53 (4), 1135–1146. [PubMed: 15306017]

(89). Li Z; Nair SK Quorum Sensing: How Bacteria Can Coordinate Activity and Synchronize Their Response to External Signals? Protein Sci. 2012, 21 (10), 1403–1417. [PubMed: 22825856]

(90). Dulcey CE; Dekimpe V; Fauvelle D-A; Milot S; Groleau M-C; Doucet N; Rahme LG; Lépine F; Déziel E The End of an Old Hypothesis: The Pseudomonas Signaling Molecules 4-Hydroxy-2-Alkylquinolines Derive from Fatty Acids, Not 3-Ketofatty Acids. Chem. Biol 2013, 20 (12), 1481–1491. [PubMed: 24239007]

(91). Pawar V; Komor U; Kasnitz N; Bielecki P; Pils MC; Gocht B; Moter A; Rohde M; Weiss S; Häussler S In Vivo Efficacy of Antimicrobials against Biofilm-Producing Pseudomonas Aeruginosa. Antimicrob. Agents Chemother 2015, 59 (8), 4974–4981. [PubMed: 26055372]

(92). Lau GW; Ran H; Kong F; Hassett DJ; Mavrodi D Pseudomonas Aeruginosa Pyocyanin Is Critical for Lung Infection in Mice. Infect Immun 2004, 72 (7), 4275–4278. [PubMed: 15213173]

(93). Winstanley C; Fothergill JL The Role of Quorum Sensing in Chronic Cystic Fibrosis Pseudomonas Aeruginosa Infections. FEMS Microbiol. Lett 2009, 290 (1), 1–9. [PubMed: 19016870]

(94). Price-Whelan A; Dietrich LE; Newman DK Pyocyanin Alters Redox Homeostasis and Carbon Flux through Central Metabolic Pathways in Pseudomonas Aeruginosa PA14. J Bacteriol 2007, 189 (17), 6372–6381. [PubMed: 17526704]

(95). Gellatly SL; Hancock REW Pseudomonas Aeruginosa: New Insights into Pathogenesis and Host Defenses. Pathog. Dis 2013, 67 (3), 159–173. [PubMed: 23620179]

(96). Dietrich LEP; Teal TK; Price-Whelan A; Newman DK Redox-Active Antibiotics Control Gene Expression and Community Behavior in Divergent Bacteria. Science (80-.). 2008, 321 (5893), 1203–1206.

(97). Kipnis E; Sawa T; Wiener-Kronish J Targeting Mechanisms of Pseudomonas Aeruginosa Pathogenesis. Médecine Mal. Infect 2006, 36 (2), 78–91.

(98). Mavrodi DV; Bonsall RF; Delaney SM; Soule MJ; Phillips G; Thomashow LS Functional Analysis of Genes for Biosynthesis of Pyocyanin and Phenazine-1-Carboxamide from Pseudomonas Aeruginosa PAO1. J. Bacteriol 2001, 183 (21), 6454–6465. [PubMed: 11591691]

(99). Li Q-A; Mavrodi DV; Thomashow LS; Roessle M; Blankenfeldt W Ligand Binding Induces an Ammonia Channel in 2-Amino-2-Desoxyisochorismate (ADIC) Synthase PhzE. J. Biol. Chem 2011, 286 (20), 18213–18221. [PubMed: 21454481]

(100). Parsons JF; Calabrese K; Eisenstein E; Ladner JE Structure and Mechanism of *Pseudomonas Aeruginosa* PhzD, an Isochorismatase from the Phenazine Biosynthetic Pathway †, ‡, §. Biochemistry 2003, 42 (19), 5684–5693. [PubMed: 12741825]

(101). Blankenfeldt W; Parsons JF The Structural Biology of Phenazine Biosynthesis. Curr. Opin. Struct. Biol 2014, 29, 26–33. [PubMed: 25215885]

(102). Ahuja EG; Janning P; Mentel M; Graebsch A; Breinbauer R; Hiller W; Costisella B; Thomashow LS; Mavrodi DV; Blankenfeldt W PhzA/B Catalyzes the Formation of the Tricycle in Phenazine Biosynthesis. J. Am. Chem. Soc 2008, 130 (50), 17053–17061. [PubMed: 19053436]

(103). Parsons JF; Calabrese K; Eisenstein E; Ladner JE Structure of the Phenazine Biosynthesis Enzyme PhzG. Acta Crystallogr. D. Biol. Crystallogr 2004, 60 (Pt 11), 2110–2113. [PubMed: 15502343]

(104). Greenhagen BT; Shi K; Robinson H; Gamage S; Bera AK; Ladner JE; Parsons JF Crystal Structure of the Pyocyanin Biosynthetic Protein PhzS †‡. Biochemistry 2008, 47 (19), 5281–5289. [PubMed: 18416536]

(105). Parsons JF; Calabrese K; Eisenstein E; Ladner JE Structure and Mechanism of Pseudomonas Aeruginosa PhzD , an Isochorismatase from the Phenazine Biosynthetic Pathway †,‡, §. 2003, 5684–5693.

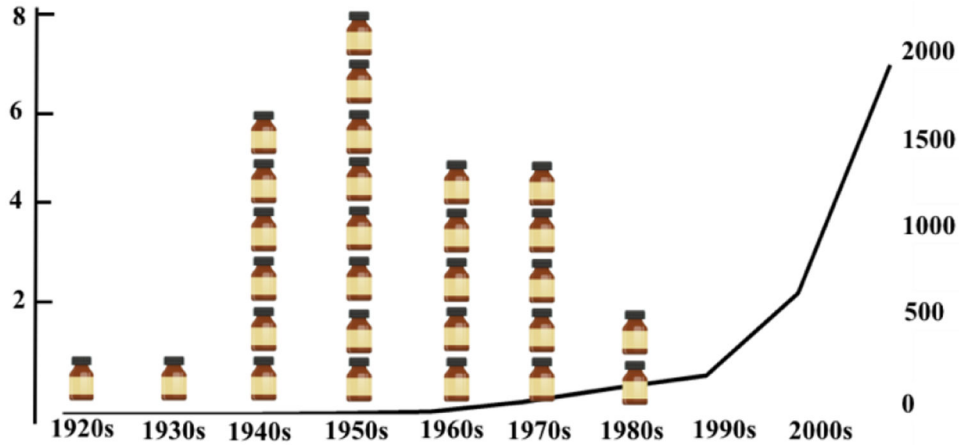

Figure 1:

"Discovery void of antibotics". Number of antibacterials drugs discovered by decade (medicine botlles) and published papers about "bacteria resistance" in pubmed [MESH terms='antibiotic resistance'[All Fields]

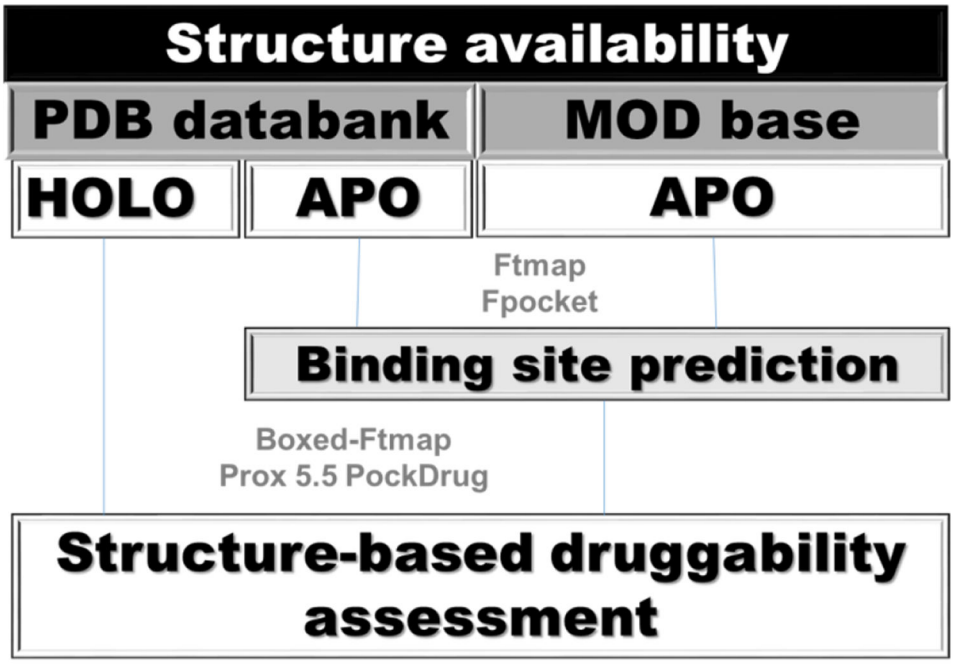

Figure 2.

In silico steps for druggability assessment of *P. aeruginosa* anti-virulence targets using pockDrug or FTmap. Boxed-FTmap indicates that probes more than 4.0 Å apart from the ligand where not considered during the in silico solvent mapping. As a consequence, only the hot spots surrounding the ligand were employed for the duggability assessment. Prox 5.5 indicates that only pockets within 5.5 Å of the ligand where considered for druggability assessment within PockDrug.

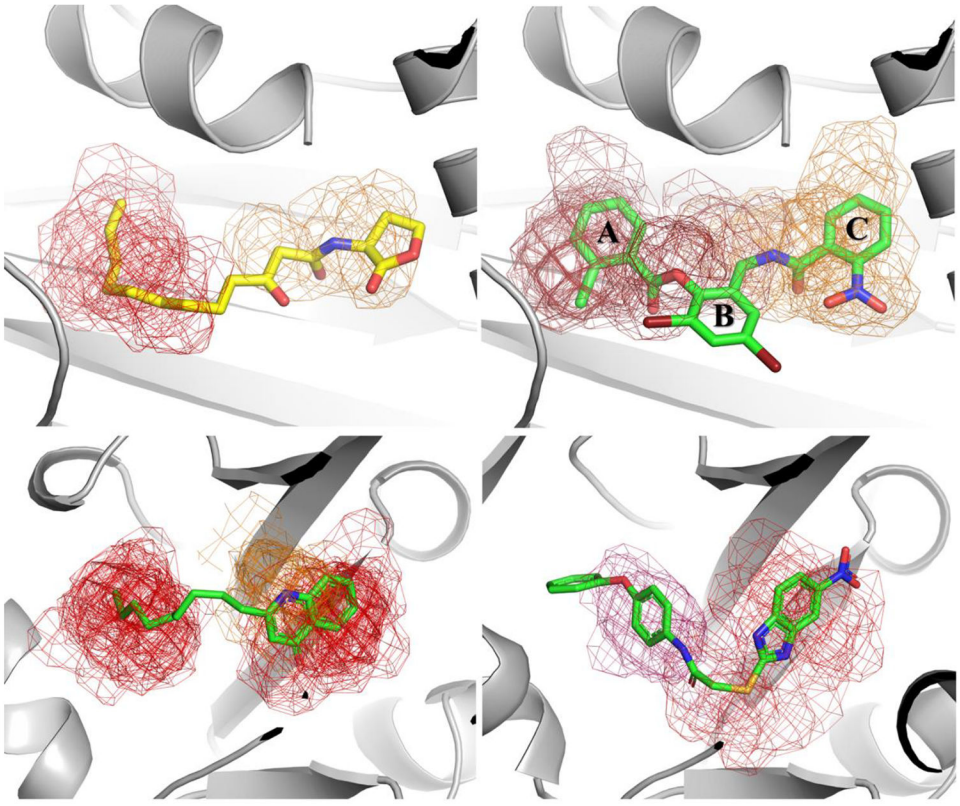

Figure 3.

Main hot spots within LasR (upper panel) and MvfR (lower panel) substrate binding sites identified by FTmap, when the search is focused around the ligand. Upper Left -The substrate alkyl chain occupies one hot spot (red mesh) that is close to a weaker consensus site (orange 12 probes). Upper right – The LasR agonist TP1 (2,4-dibromo-6-({[(2-nitrophenyl)carbonyl]amino}methyl)phenyl 2-chlorobenzoate) reaches two hot spots that are close to each other (red). In addition, there is a weaker consensus site (orange 8 probes) bridging the hot spots. Lower left -The substrate alkyl chain occupies one hot spot whereas the quinolone ring binds the second hot spot within the binding site (red mesh). Lower right – The conformational rearrangement caused by MvfR antagonist 2-[(5-nitro-1H-benzimidazol-2-yl)sulfanyl]-N-(4-phenoxyphenyl)acetamide (M64) reveals additional connected hot spots (red-warm pink mesh), within the substrate binding site, that are completely fulfilled by this compound.

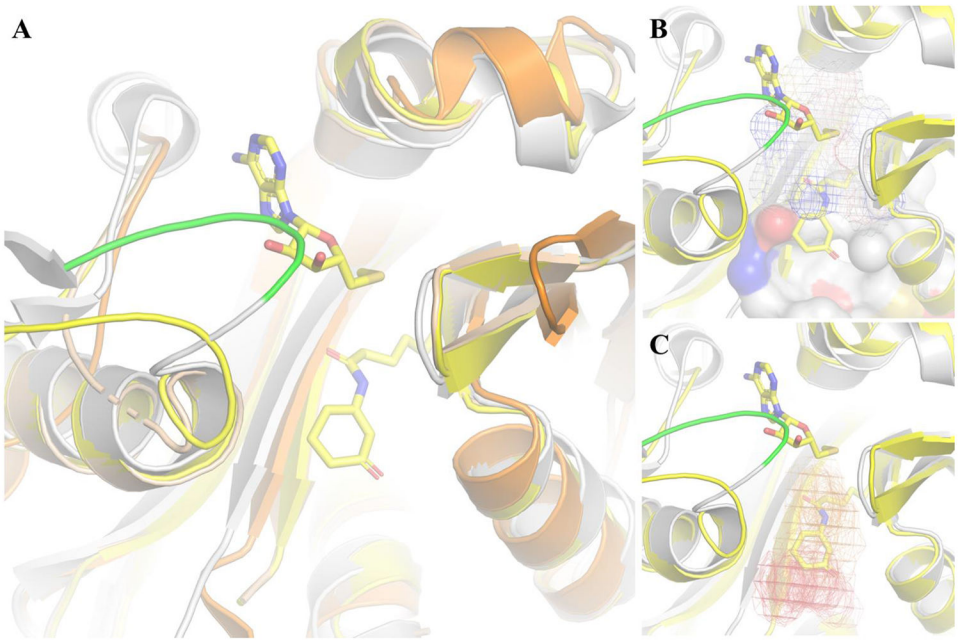

Figure 4:

Structural insights to develop LasI inhibitors. A) Overlay of LasI (gray), EsaI (orange), TofI-HOLO (yellow) and TofI-APO (wheat) reveals that the LasI SAM binding site is occluded by loop 30-36 (green); B) Pockdrug predicted pockets (P0 surface, P1 mesh) that line the substrate binding site; C) The first two consensus sites (red and orange mesh, respectively) from FTmap, which allow for drug-like molecules to bind to LasI, overlap with Acyl-ACP binding site. No Consensus Site was observed in SAM binding site due to steric clashes with loop 30-36 (green).

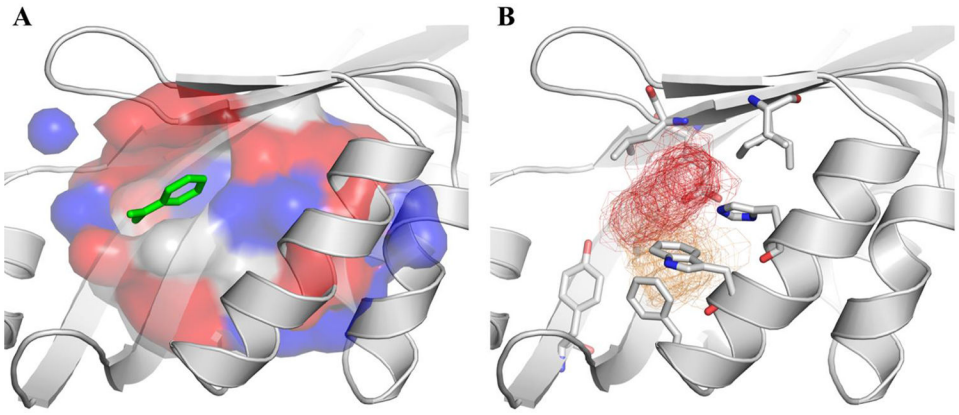

Figure 5.

Druggability assessment of *P. aeruginosa* PhzB active site. A) Central cavity where the substrate is expected to bind. B) Hot spots (red and orange mesh) found within the central cavity allow drug-like molecules to form H-bonds and hydrophobic interactions to surrounding residues.

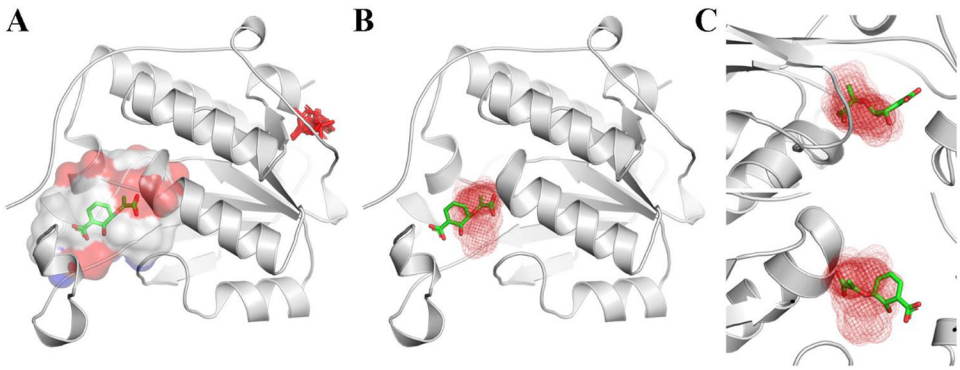

Figure 6.

PhzD binding site druggability assessment. A) FTmap does not find hotspots with more than 16 probes in PhzD active site, if default parameters are employed; B) Druggable hotspot identified by FTmap when the coordinates of the active site are provided (boxed-FTmap); C) Zoomed views of the hotspot overlaid on the ligand from the mutant PhzD.

Table 1:

Structure-based druggability assessment of anti-virulence targets responsible for QS modulation in *P. aeruginosa*, according to FTmap and Pockdrug servers.

Target	PDB ID/MODBASE	Resolution or Template (identity %)	FTmap druggability	Ligand
LasR	3IX3	1.4	DPM	OHN
	3IX4	1.8	D	TX1
	3JPU		D	TY4
RhlR	A0A086C1L6	4LFU (41)	D	-
MvfR (PqsR)	4JVC	2.5	DPM	-
	4JVD	2.95	D	NNQ
	4JVI	2.95	BD	QZN
	6B8A	2.65	D	CZG
PscR	6CBQ	2.8	DPM	EVY
	6CC0	2.5	BD	EWM
	3SZT	2.55	D	OHN
Target	**PDB ID/MODBASE**	**PockDrug druggability score***		**Ligand**
LasR	3IX3	0.98 ± 0.0		OHN
	3IX4	0.99 ± 0.0		TX1
	3JPU	0.98 ± 0.0		TY4
RhlR	A0A086C1L6	0.94 ± 0.02		-
MvfR (PqsR)	4JVC	0.94 ± 0.02		-
	4JVD	1.0 ± 0.0		NNQ
	4JVI	0.99 ± 0.0		QZN
	6B8A	0.98 ± 0. 0		CZG
QscR	6CBQ	0.99 ± 0.0		EVY
	6CC0	0.99 ±0.01		EWM
	3SZT	0.98 ± 0.01		OHN

*Only the main binding site (P0) was considered for apo structures or homology models (highlighted in gray)

Table 2-

Structure-based druggability assessment of enzymes responsible for autoinducers synthesis in *P. aeruginosa*, according to FTmap and Pockdrug servers

Target	PDB ID/MODBASE	Resolution or Template (identity %)	FTmap ligandability	Ligand
LasI	1RO5	2.3	D	-
RhlI	P54291	3P2H (38)	DPM	-
PqsA	5OE6	1.67	D	9SN
PqsBC	5DWZ	2.04	DPM	-
PqsD	3H76	1.8	D	-
	3H77	1.8	D	COW
PqsE	3DH8	1.8	D	B4N
	5HIO	1.9	BD	61M
	5HIP	1.99	D	61O
	5HIS	1.77	N	60P
Target	**PDB ID/MODBASE**	**PockDrug druggability score***		**Ligand**
LasI	1RO5	1.0 ± 0.0		-
RhlI	P54291	0.5 ± 0.02		-
PqsA	5OE6	0.89 ± 0.04		9SN
PqsBC	5DWZ	0.89 ± 0.02		-
PqsD	3H76	0.9 ± 0.01		-
	3H77	0.8 ±0.04		COW
PqsE	3DH8	0.73 ± 0.18		B4N
	5HIO	0.6 ± 0.21		61M
	5HIP	0.82 ± 0.17		61O
	5HIS	0.56 ± 0.21		60P

*Only the main binding site (P0) was considered for apo structures or homology models (highlighted in gray)

Table 3-

Structure-based druggability assessment of enzymes responsible for pyocyanin biosynthesis in *P. aeruginosa*, according to FTmap and Pockdrug servers

Target	PDB ID/MODBASE	Resolution or Template (identity %)	FTmap Druggability	Ligand
PhzA	Q9HWH1.1	3JUM (55%)	D	-
PhzB	3FF0	1.9	D	-
PhzC	A3KTA5	5E5G(41%)	BD	-
PhzD	1NF9	1.5	DPM	-
	1NF8#	1.6	D	ISC
PhzE	A3L7X4	3R75 (55%)	BPM	-
PhzG	1TY9	1.8	BD	-
PhzM	2IP2	1.8	BD	-
PhzS	3C96	1.9	D	-
Target	**PDB ID/MODBASE**	**PockDrug druggability score***		**Ligand**
PhzA	Q9HWH1.1	0.83 ± 0.07		-
PhzB	3FF0	0.9 ± 0.07		-
PhzC	A3KTA5	0.01 ± 0.0		-
PhzD	1NF9	0.86 ± 0.07		-
	1NF8#	0.92 ± 0.09		ISC
PhzE	A3L7X4	0.79 ± 0.06		-
PhzG	1TY9&	0.92 ± 0.02		-
PhzM	2IP2	0.96 ± 0.0		-
PhzS	3C96	0.73 ± 0.03		-

*Only the main binding site (P0) was considered for apo structures or homology models (highlighted in gray);

#Mutated protein

&decoy pocket with 10-14 residues